

An Experimental and Numerical Study of Low Velocity Impact of Unsaturated Polyester/Glass Fibre Composite

Sanita ZIKE¹, Kaspars KALNINS^{1*}, Olgerts OZOLINS¹, Maris KNITE²

¹Institute of Materials and Structures, Riga Technical University, Azenes street 16/20-323, Riga, LV-1048, Latvia

²Institute of Technical Physics, Riga Technical University, Azenes street 12/24-321, Riga, LV-1048, Latvia

crossref <http://dx.doi.org/10.5755/j01.ms.17.4.773>

Received 22 November 2010; accepted 02 February 2011

In this paper validation of experimental and numerical results of low-velocity impact tests of unsaturated polyester/glass fibre composite laminate has been carried out. Impact response of composite laminates was experimentally studied with drop-tower Instron 9250HV determining impact force, energy absorption and deflection. In addition, quasi-static testing equipment Zwick Z100 has been used to determine material mechanical properties to ensure good input data for numerical predictions. Numerical model has been created with the finite element commercial code ANSYS/LS-DYNA to simulate impact response of composite laminate. Also non-destructive ultrasonic B- and C- scan imagining with USPC 3010 system has been used to identify the deformation regions in the specimens and compare to simulation results. During the impact test all samples were perforated, showing brittle response followed by matrix cracking and delamination. Overall good agreement between experimental and simulation results was achieved, comparing impact characterizing parameters as load, energy and deflection. Discrepancy has been observed between ultrasonic scanning and simulation code ANSYS/LS-DYNA results of rupture and delamination. Simulation shows less uniform and larger deformation than it was experimentally observed.

Keywords: low velocity impact, plate impact, composite, simulation, glass fibre composite, C-scan, B-scan.

1. INTRODUCTION

The highly specific mechanical properties of composite laminates is leading to increased usage in a number of engineering fields such as the aircraft, railroad, automotive and marine industry by replacing metal alloy structural elements. Drawback of polymer/glass or carbon fibre composites compared to metal alloys are more brittle and elastic deformation followed by fibre fracture, matrix cracking, fibre-matrix de-bonding and delamination, also laminates poorly resist and dissipate impact energy in transverse direction [1, 2]. Therefore impact loading represents a concern for usage of laminated composites in fields as crashworthiness [3], ballistics and in-service application [4].

Furthermore structural materials can be subjected to complex loading configurations, thus prototyping and experimental testing in order to evaluate the mechanical response can be expensive and time consuming process. Therefore more often simulation codes are applied by industry to optimise the performance of the composite material response during in service load. Most common commercial simulation codes used to predict impact properties are LS-DYNA, ABAQUS, PAM-CRASH, 3DIMPACT etc. [4–8]. General purpose finite element code LS-DYNA is one of the most frequently used commercial codes in crash test simulations by the automotive industry, as well as in aerospace, metal forming, material processing, sport, biomedical and other industries [6, 9].

Moreover the proper prediction of structural materials depends on defined boundary conditions, loads and material definition. Available laminated composite models in LS-DYNA are described by Schweizerhof [10] and Hallquist [9]. Thus common material models of composite laminates used for impact response prediction in LS-DYNA are Mat_22_Composite damage [11,12], Mat_54/55_Enhanced composite damage [6], Mat_58_Laminated composite fabric [13] and Mat_161/162_Composite MSC [14]. Material models Mat_22 and Mat_54 are based on Chang-Chang failure criteria. Mat_54 being an enhanced version of Mat_22 introduces stress and strain limiting parameters, which facilitate better validation with experimental results [10]. Therefore material models Mat_58 and Mat_161/162 are based on criteria developed from methodology of Hashin [9]. Comparing to other models Mat_161/162 allows simulation of delamination.

The aim of this work is to study the agreement between the experimentally determined and numerically predicted impact properties of unsaturated polyester/glass fibre composite. Validation model has been worked out using experimentally performed low-velocity impact test compared to simple plate impact simulation model set in ANSYS/LS-DYNA. Furthermore this information can be used to simulate more complex and large scale structures. Therefore this paper involves discussion about experimentally determined impact response character of unsaturated polyester/glass fibre composite, composite material simulation capabilities in non-linear finite element program LS-DYNA, also implementation of non-destructive ultrasonic scanning method to evaluate rupture and delamination area of laminated composites and comparison to numerical simulation results.

*Corresponding author. Tel.: +371-267-51614; fax.: +371-670-89254.
E-mail address: kaspars.kalnins@sigmanet.lv (K. Kalnins)

2. EXPERIMENTAL TESTS

2.1. Specimen manufacturing

Composite laminates were made of orthophthalic polyester POLYLITE 440-M888 resin and glass fibre fabric AERO having an areal density of 80 g/m². POLYLITE was mixed with 1.5 % Norpol Peroxide to initiate free radical polymerization and cross-bonding of polyester molecules with styrene. Composite laminate of fourteen glass fabric layers with equal stacking sequence and total thickness of 1.3 mm has been made by hand lay-up processing method at room temperature.

2.2. Determination of mechanical properties

Mechanical properties of composite were obtained with a quasi-static testing equipment Zwick Z100 employing 100 kN load cell with test data acquisition rate of 10 Hz. In order to determine tensile and shear modulus and Poisson ratio (according to ASTM standards D3039 and D3518) HBM strain gauges 6/350E LY4/S-3 were used. The dimensions of specimens were 250 mm × 25 mm and gauge length 100 mm. Applied testing speed was 2 mm/min for tensile and 5 mm/min for shear properties determination. Obtained average mechanical properties of the composite specimens are summarized in the Table 1.

Table 1. In plane mechanical properties of composite material

Property, unit	Value
Tensile strength (90°), MPa	130 ±5
Young's modulus (90°), GPa	11.6 ±0.5
Shear strength, MPa	38 ±1
Shear modulus, GPa	3 ±0.15
Tensile strength (0°), MPa	164 ±5
Young's modulus (0°), GPa	13.7 ±0.4
Poisson's ratio	0.15 ±0.02

2.3. Impact testing

The low velocity impact tests were performed by drop tower INSTRON Dynatup 9250HV. During test impact machine was equipped with a hemispherical 15.6 kN indenter with diameter of 10 mm. Specimens with dimensions of (100 × 100) mm ±5 mm were fixed in pneumatic clamping system with inner ring diameter of 76.2 mm. Impact velocity was set to 2.04 m/s to provide resultant impact energy of 14 J.

2.4. Ultrasonic scanning

The non-destructive ultrasonic imaging (NDUI) system USPC 3010 was used to analyze impacted region and delamination growth of specimens. The system consisted of a computer-controlled ultrasonic flaw detector USPC 3010 Industrial, an immersion ultrasonic probe of 10 MHz, a glass water tank, and a stepper motor-controlled XYZ-manipulator. Ultrasonic scanning was done both in plane and thickness direction therefore C and B scans were

performed. C-scan results were distinguished in flaw echo and back wall scanning showing the top and bottom surfaces of the specimens, respectively.

3. NUMERICAL SIMULATION

3.1. Design of material model

Impact specimens were modelled using shell elements with equal distribution of 14 integration points corresponding to each layer. Impact energy, velocity and indenter diameter, sample constraints were set accordingly to experimental test. As shown in Fig. 1 simulation include initial velocity direction and node rotational and translational constraints in 38 mm radius from centre. Indenter is modelled as rigid ball using material model MAT22_Rigid.

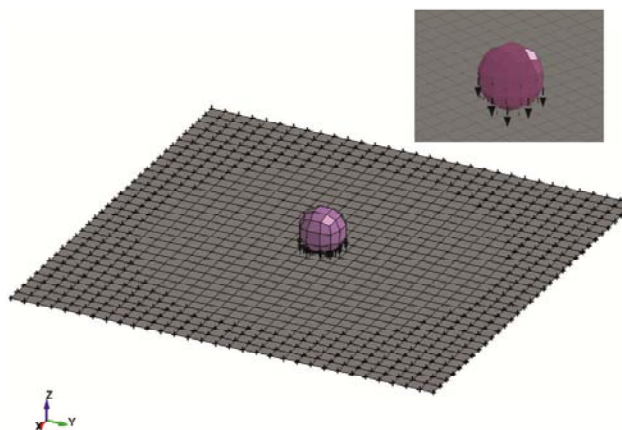


Fig. 1. Model used for simulation

3.2. Applied material models

LS-DYNA offers several material models for simulation of composite materials response. In this research material model MAT 54 is discussed as enhanced version of model MAT 22 [9], as it showed better agreement with the experimental results. Simulation results using these material models are given by Heimbs et al. [6], Iannucci et al. [11] and Griškevičius et al. [12] in all cases showing good agreement. Material model 54 and 22 are based on Chang-Chang failure criteria. Criteria define material failure or elastic response of fibre and matrix in tensile or compressive mode depending on applied load. Element is deleted when failure criteria has been fulfilled. Equations of failure criteria are available in Theory manual of LS-DYNA [9].

Beside mechanical properties used in MAT 54 [9] additional strain limiting and stress softening parameters can be used to enhance agreement between simulation and experimental results. Strain limiting parameters allow transition from linear-brittle to elasto-plastic behaviour of material. This means, during deformation after reaching the maximum stress in fibre direction, the stress remains constant until the maximum strain is reached [9, 10]. Strain limiting parameters used in this study – maximum strain for fibre tension (DFAILT) was set to 0.04; maximum strain for fibre compression (DFAILC) –0.035; maximum strain for matrix (DFAILM) 0.2 and maximum shear strain

(DFAILS) 0.13. Stress softening parameters are used to predict reduction of mechanical properties as Young's modulus, tensile and compressive strength after neighbored elements have been failed. In this study stress softening parameters were not used.

4. RESULTS AND DISCUSSION

A low velocity impact test has been carried out to determine impact response of unsaturated polyester/GF composite. Experimentally determined results are compared to ANSYS/LS-DYNA simulation results using impact response characterizing parameters as load, energy and deflection. In addition impact induced deformation as rupture and delamination has been analyzed by non-destructive ultrasonic visual method and compared to simulation results.

4.1. Evaluation of experimental results

Experimentally determined data were uniform showing high conformity between parallel specimens, therefore agreement between load vs. deflection curves of five parallel specimens is shown in Fig. 2. In load vs. deflection curves almost coincident data were observed in ascending part related to bending stiffness or material capability to resist impact force in flexure. This suggests that materials are enough homogeneous. Furthermore material can be characterized by maximum force and descending part. Maximum force shows the force needed to induce composite damage through matrix cracking, delamination and fibre fracture. The average observed maximum force with small dispersion was 0.8 kN (Fig. 2). The highest disagreement was observed in descending part of the load-displacement curve what is due to non-similarities in impact stress dissipation and delamination evolution.

Moreover impact curves of experimentally tested specimens were open type typical to perforated materials otherwise curves would be closed type when curves bend inwards force-deflection curve because of recovering elastic bending deformation (Fig. 2) [15–17].

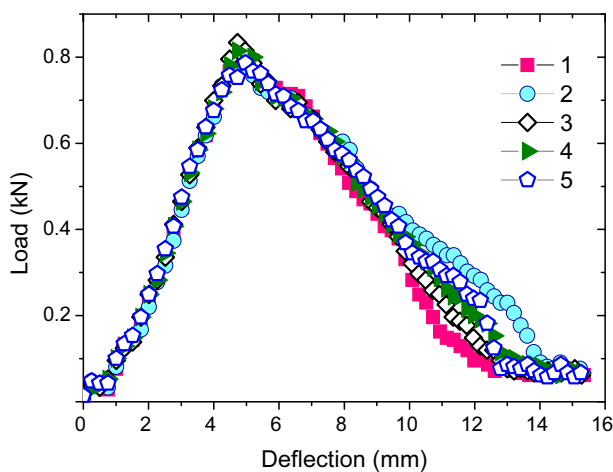


Fig. 2. Impact load vs. deflection

Average absorbed energy is equal to perforation energy 5.5 J as all the specimens were perforated. The

absorbed energy of material can be determined as shown in Fig. 3, where absorbed energy curve is compared to impact force curve. The perforated energy was acquired at the perforation point on load curve, where the load values reach the minimum in the descending part. After reaching the value of perforation energy the energy–time curve is continuing to rise due to the friction at the edges of the perforation hole against the lateral surface of the indenter [18].

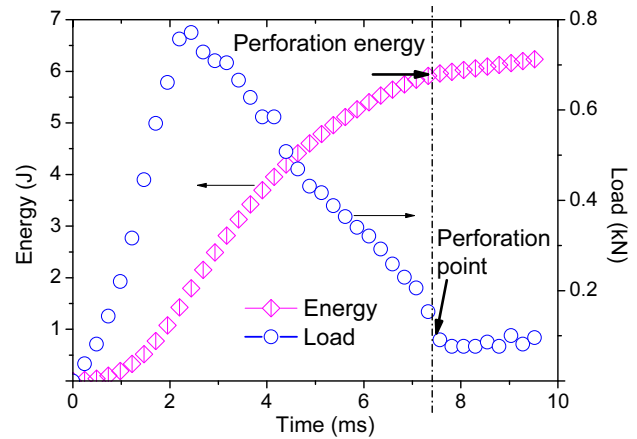


Fig. 3. Determination of perforation energy

4.2. Validation of experimental results with simulation

Similar data to experimental were collected during low-velocity impact simulation with ANSYS/LS-DYNA (Fig. 4). Impact load shows some deviations in ascending part from the experimental data is explained by small disagreement in bending stiffness prediction. In descending part good agreement was observed as predicted results were very close to dissipated results of experimental tests. Even though calculations implemented in material model Mat_54 used in this study did not include delamination what provides the gradual decrease of impact force in load vs. deflection curve [9]. Therefore appearance of gradual decrease of force was suggested to be related to the strain limiting parameters which allow modifications of deformation.

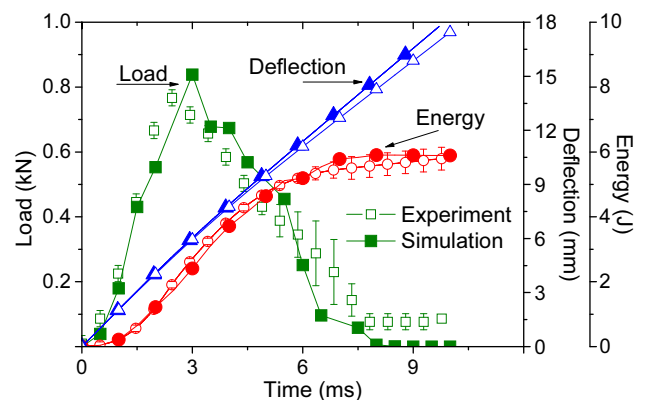


Fig. 4. Conformity of impact load, energy and deflection between simulation and experimental data

As it was discussed previously, in the experimental tests after perforation of material energy continues increase

and impact forces remain constant at values higher than zero due to sufficient friction. Contrary to the experimental results in simulation predicted results impact force reaches the zero values and energy remains fixed as friction was not included in simulation model [15]. Moreover conformity of absorbed energy and displacement between simulation and experimental results shows good agreement (Fig. 4). Small dissimilarities observed within displacement and energy curve can be explained with the same reasons as in load–time curve.

Furthermore Heimbs et al. [6] showed good results simulating carbon fibre/epoxy resin composites pre-loaded in compression using material model Mat 54. Similar to this study the main dissimilarities were observed in damage evolution regions around force peak. Close agreement between simulation and experimental results are also achieved by Sevkat et al. [16] using user defined material model in LS-DYNA to predict hybrid composite laminate response to low-velocity impact.

4.3. Visual inspection of impact results

Visual inspection of materials with non-destructive ultrasonic scanning method was used to evaluate rupture and delamination and also to compare experimental and simulation results. Conformity of deformation is of the same importance as prediction of load, energy and deflection, when transition from small to large scale has been done.

Photograph and ultrasonic scanning results represented in Figs. 5–6 show that impacted specimens have a rhombus-shape delamination area. The character of delamination pattern is dependent on the structure of the fabric, thus it is more pronounced in fibre direction, and has lower extent between fibres as interlaced yarns restrict the growth of delamination. Shy and Pan [18] had discussed the influence of fibre orientation in unsaturated polyester/glass fibre laminated composites on delamination growth. Moreover all specimens showed relatively large cone shape indentation of puncture as it is shown in the photograph of Fig. 5.

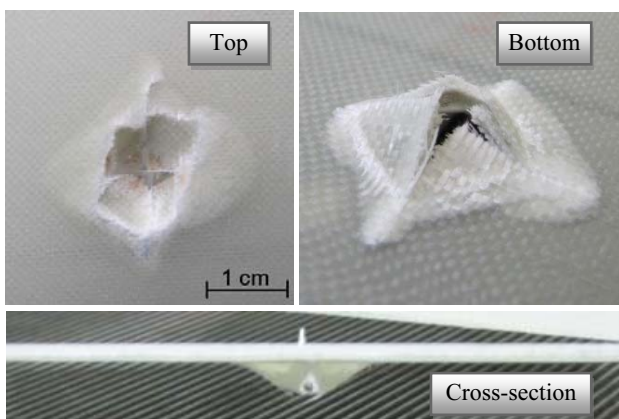


Fig. 5. Top, bottom and cross-section photograph of tested specimen

In Fig. 6 flaw echo and back wall scanning results are presented, which describe scanning results from top and bottom surface, respectively. Drawback comparing to the photograph is that delamination can be fully evaluated with

two back wall and flaw echo pictures instead of one, while the rupture can be clearly distinguished in both pictures of Fig. 6 characterized by the highest loss of sound [6, 16, 19, 20]. NDUI system is crucial in the fields where analyzes of non-transparent material deformation is done [20].

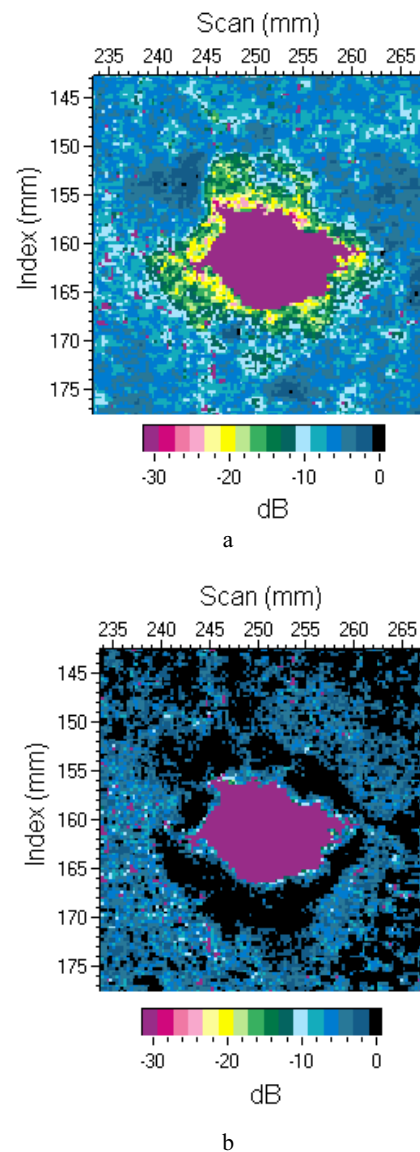


Fig. 6. NDUI C-scan results: a – back wall; b – flaw echo

Moreover B-scan can be very useful to analyze deformation evolution in the thickness. The results of B-scan are given in the Fig. 7 where top and bottom surfaces can be distinguished by upper dark and the lowest light line, respectively.

Fig. 7 shows three different parts of one impacted specimen corresponding to non-deformed, delamination and rupture with delamination region. The NDUI B-scan cross-sectional results of delamination and rupture region agree well with the C-scan in plane scanning results. For example, in Fig. 7, c, the range of delamination is given from 250 mm till 280 mm and rupture from 262 mm till 272 mm, so the differences are about 30 mm and 10 mm. These results can be compared to more precisely summarized C-scan data in Figs. 8–9. The B-scan results

showed uniform delamination through the thickness in all tested specimens.

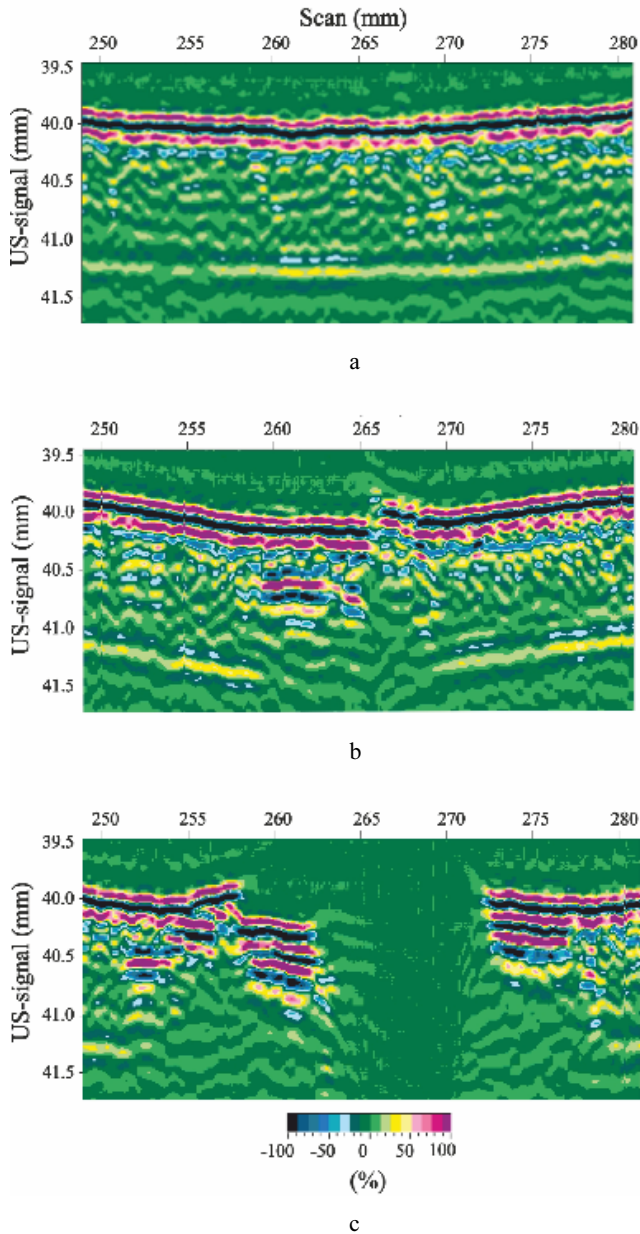


Fig. 7. NDUI B-scan results: a – not deformed; b – delamination; c – delamination and rupture

Furthermore with NDUI system obtained results were placed in coordinate system, where the zero point is equal to the puncture centre. This method allows better evaluate agreement between different specimens and simplifies comparison to simulation results (Figs. 8–10). During impact tests all specimens were perforated by indenter showing larger rupture diameter than indenter tip and large delamination region. The average experimental values of the ruptured region are ± 6 mm in x axis and ± 8 mm in y . The rupture regions were quite broadly dispersed what can be seen also in Fig. 8. Indenter tip diameter is 10 mm, so the rupture regions are quite larger, it could be explained due to crack appearance and growth during impact.

In the same way results of delamination were summarized in Fig. 9. Delamination amount is uniform in 0° and

90° direction which corresponds to fibre direction – about ± 14 mm in x and y axis. It should be noted that mechanical properties of material in plane direction 0° and 90° were not the same as it was shown in Table 1. Also rhombus-shape of delamination appears to be more pronounced in coordinate system therefore it can be seen that delamination amount between x and y axis is quite smaller than in direct x or y axis direction.

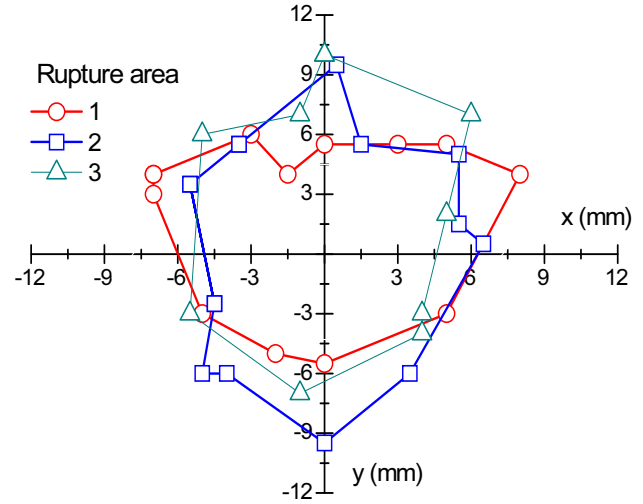


Fig. 8. C-scan rupture results of three parallel specimens placed in coordinate system

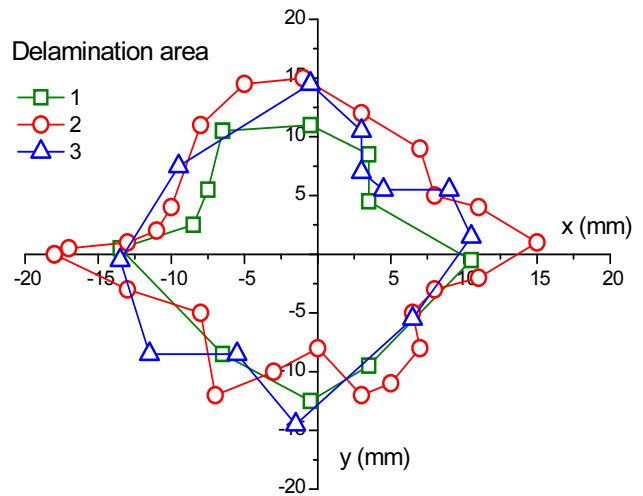


Fig. 9. C-scan delamination results of three parallel specimens placed in coordinate system

4.4. Comparison of NDUI with simulation results

Results of visual inspection of materials with NDUI were compared with the calculation of simulation code. LS-DYNA shows much higher degree of rupture in x axis ± 13 mm and smaller in y direction – ± 5.5 mm. In general material rupture appeared just in x direction, in transverse direction very pronounced bending can be observed, see Fig. 10.

Furthermore material model used in this study did not provide delamination calculation, therefore cannot be compared to delamination results measured by the NDUI. Instead of that in Fig. 11 the stress distribution during

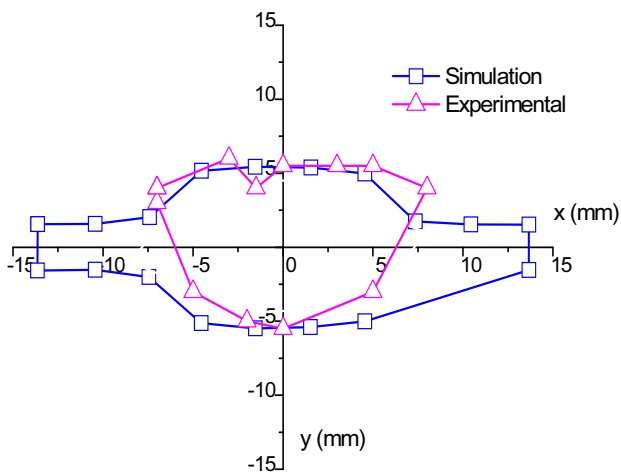


Fig. 10. C-scan and simulation results of rupture

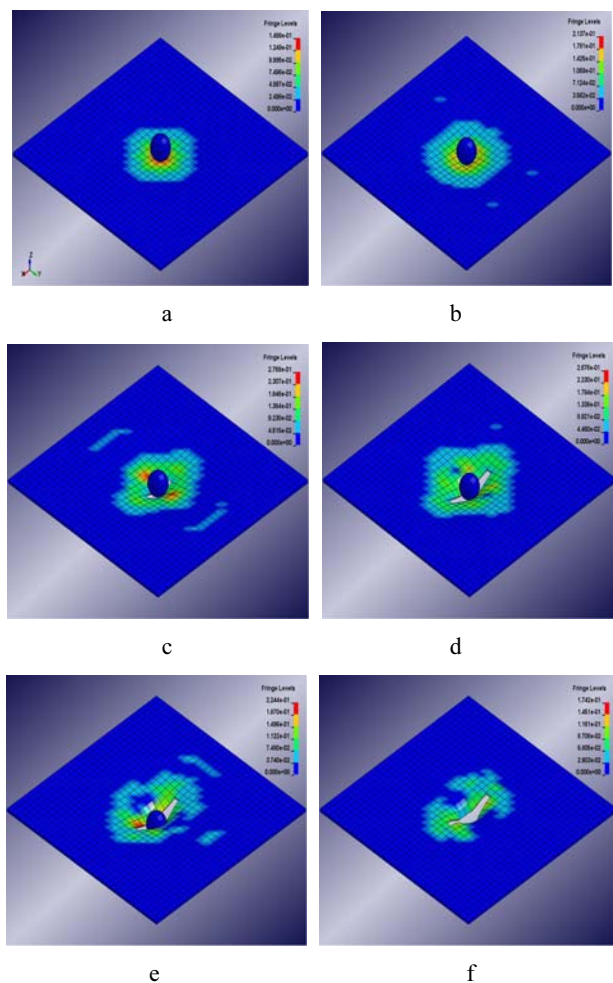


Fig. 11. Dissipation of stresses in simulation model: a – 1 ms; b – 2 ms; c – 3 ms; d – 4 ms; e – 6 ms; f – 10 ms

impact in different time intervals is shown. Stress distribution can give some important information as delamination is explained with stress accumulation between separate layers. In Fig. 11 first two steps show the bending of the plate with applied impact force what induces uniform stress dispersion. Later at 2 ms composite damage occurs in compliance with experimental results achieving limit of material strength characterized with maximum force (Fig. 2). At this point formation of stress distribution in

rhombus shape was observed and agrees with experimentally determined delamination (Figs. 5–6). Stress distribution between 3 ms and 4 ms was observed in the range of 35 mm–48 mm and 45 mm–51 mm in x and y direction, respectively. Stress distribution predicted by simulation code LS-DYNA was much higher than experimentally observed delamination of composite laminates.

CONCLUSIONS

During experimental tests determined average absorbed energy was equal to 5.5 J what was two times lower than impact energy. Also determined impact force values were relatively low – 0.8 kN. Experimental results between parallel specimens showed good agreement, some deviations were observed after inducing composite material breakage where dominant processes are related to deformation evolution. Tested specimens showed large rupture and delamination regions, where the rupture region was about 1.5 times larger than indenter tip.

Good validation of simulation and experimental results were achieved applying LS-DYNA material model Mat 54 using additional strain and stress limiting parameters. Values of predicted absorbed energy, impact force and deflection were similar to experimental, whereas worse conformity was achieved comparing rupture and delamination results. Rupture and delamination measured with non-destructive ultrasonic method of experimental results showed more uniform and smaller values than it was predicted with ANSYS/LS-DYNA.

Acknowledgments

This work was partly supported by the Latvia Council of Science grant 09.1262 "Innovative design methodology for manufacturing of composite structures with physical validation".

REFERENCES

1. **Staab, G. H.** *Laminar Composite Materials*. Butterworth Heinemann, 1999.
2. **Matzenmiller, A., Lubliner, J., Taylor, R.** A Constitutive Model for Anisotropic Damage in Fiber Composites *Mechanics of Materials* 20 1995: pp. 125–152.
3. **Jacob, G. C., Fellers, J. F., Simunovic, S., Starbuck, J. M.** Energy Absorption in Polymer Composites for Automotive Crashworthiness *Journal of Composite Materials* 36 2002: pp. 813–850.
4. **Wang, S.-X., Wu, L.-Z., Ma, L.** Low-velocity Impact and Residual Tensile Strength Analysis to Carbon Fiber Composite Laminates *Materials and Design* 31 (1) 2010: pp. 118–125.
5. **Karakuzu, R., Erbil, E., Aktas, M.** Impact Characterization of Glass/epoxy Composite Plates: An Experimental and Numerical Study *Composites Part B: Engineering* 41 (7) 2010: pp. 388–395.
6. **Heimbs, S., Heller, S., Middendorf, P., Hähnel, F., Weiße, J.** Low Velocity Impact on CFRP Plates with Compressive Preload: Test and Modelling *International Journal Impact Engineering* 36 (10) 2009: pp. 1182–1193. <http://dx.doi.org/10.1016/j.ijimpeng.2009.04.006>

7. **Lopes, C. S., Camanho, P. P., Gürdal, Z., Maimí, P., González, E. V.** Low-velocity Impact Damage on Dispersed Stacking Sequence Laminates. Part II: Numerical Simulations *Composite Science Technology* 69 (6) 2009: pp. 937–947.
8. **Tita, V., Decarvalho, J., Vandepitte, D.** Failure Analysis of Low Velocity Impact on Thin Composite Laminates: Experimental and Numerical Approaches *Composite Structures* 83 (6) 2008: pp. 413–428.
9. **Hallquist, J. O.** Theory Manual of LS-DYNA. Livermore Software Technology Corporation, 2006.
10. **Schweizerhof, K., Weimar, K., Munz, T., Rottner, T.** Crashworthiness Analysis with Enhanced Composite Materials Models in LS-DYNA – Merits and Limits *Proceedings of the LS-DYNA World Conference* Detroit, USA, 1998: pp. 1–17.
11. **Iannucci, L., Willows, M. L.** An Energy Based Damage Mechanics Approach to Modelling Impact onto Woven Composite Materials – Part I: Numerical Models *Composite Part A: Applied Science and Manufacturing* 37 (11) 2006: pp. 2041–2056.
<http://dx.doi.org/10.1016/j.compositesa.2005.12.013>
12. **Griškevičius, P., Zeleniakienė, D., Leišis, V., Ostrowski, M.** Experimental and Numerical Study of Impact Energy Absorption of Safety Important Honeycomb Core Sandwich Structures *Materials Science (Medžiagotyra)* 16 2010: pp. 119–123.
13. **Magistrali, S., Perillo, M.** Calibration and Experimental Validation of LS-DYNA Composite Material Models by Multi Objective Optimization Techniques *Proceedings of the 9th International LS-DYNA Conference* Michigan, USA, 2006: pp. 17–24.
14. **Brown, K., Brooks, R., Warrior, N.** Numerical Simulation of Damage in Thermoplastic Composite Materials *Proceedings of the 5th European LS-DYNA Users Conference* 2005: pp. 5d–47.
15. **Sayer, M., Bektaş, N. B., Sayman, O.** An Experimental Investigation on the Impact Behavior of Hybrid Composite Plates *Composite Structures* 92 (4) 2010: pp. 1256–1262.
16. **Sevkat, E., Liaw, B., Delale, F., Raju, B. B.** Drop-weight Impact of Plain-woven Hybrid Glass–graphite/toughened Epoxy Composites *Composite Part A: Applied Science and Manufacturing* 40 (8) 2009: pp. 1090–1110.
<http://dx.doi.org/10.1016/j.compositesa.2009.04.028>
17. **Atas, C., Sayman, O.** An Overall View on Impact Response of Woven Fabric Composite Plates *Composite Structures* 82 (2) 2008: pp. 336–345.
18. **Shyr, T.** Impact Resistance and Damage Characteristics of Composite Laminates *Composite Structures* 62 (11) 2003: pp. 193–203.
19. **Zike, S., Kalnins, K., Ozolins, O.** Experimental Verification of Simulation Model of Impact Response Tests for Unsaturated Polyester/GF and PP/GF Composites *Computer Methods in Materials Science* 11 (1) 2011: pp. 88–94.
20. **Hufenbach, W., Gude, M., Ebert, C.** Hybrid 3D-textile Reinforced Composites with Tailored Property Profiles for Crash and Impact Applications *Composite Science Technology* 69 2009: pp. 1422–1426.
21. **Kalnins, K., Rikards, R., Auzins, J., Bisagni, C., Abramovich, H., Degenhardt, R.** Metamodeling Methodology for Postbuckling Simulation of Damaged Composite Stiffened Structures With Physical Validation *International Journal Structural Stability and Dynamics* 10 2010: pp. 705–716.

*Presented at the International Conference
"Baltic Polymer Symposium 2010"
(Palanga, Lithuania, September 8–11, 2010)*